

Detection near 1-nm with a laminar-flow, water-based condensation particle counter

Susanne V. Hering^a, Gregory S. Lewis^a, Steven R. Spielman^a, Arantzazu Eiguren-Fernandez^a, Nathan M. Kreisberg^a, Chongai Kuang^b, and Michel Attoui^c

^aAerosol Dynamics Inc., Berkeley, California, USA; ^bBrookhaven National Laboratory, Upton, New York, USA; ^cLisa Université Paris Est Créteil, Paris, France

ABSTRACT

Presented is a laminar-flow, water-based condensation particle counter capable of particle detection near 1 nm. This instrument employs a three-stage, laminar-flow growth tube with a “moderator” stage that reduces the temperature and water content of the output flow without reducing the peak supersaturation, and makes feasible operation at the large temperature differences necessary for achieving high supersaturations. The instrument has an aerosol flow of 0.3 L/min, and does not use a filtered sheath flow. It is referred to as a “versatile” water condensation particle counter, or vWCPC, as operating temperatures can be adjusted in accordance with the cut-point desired. When operated with wall temperatures of $\sim 2^{\circ}\text{C}$, $>90^{\circ}\text{C}$, and $\sim 22^{\circ}\text{C}$ for the three stages, respectively, the vWCPC detects particles generated from a heated nichrome wire with a 50% efficiency cut-point near 1.6 nm mobility diameter. At these operating temperatures, it also detects 10–20% of large molecular ions formed from passing filtered ambient air through a bipolar ion source. Decreasing the temperature difference between the first two stages, with the first and second stages operated at 10 and 90°C , respectively, essentially eliminates the response to charger ions, and raises the 50% efficiency cut-point for the nichrome wire particles to 1.9 nm mobility diameter. The time response, as measured by rapid removal of an inlet filter, yields a characteristic time constant of 195 ms.

ARTICLE HISTORY

Received 14 September 2016
Accepted 7 November 2016

EDITOR

Jinkun Jiang

Introduction

The study of particle nucleation in the atmosphere and in laboratory settings has driven interest in detection of particles at the onset of their formation. While mass spectrometry has enabled the study of molecular clusters, there remains a gap between the largest clusters measurable by mass spectrometry and the particle size threshold of commonly available condensation particle counters (CPCs). The laminar-flow butanol-based ultrafine CPC designed by Stolzenburg and McMurry (1991) coupled to scanning mobility systems has been widely used for many years to characterize atmospheric nucleation events. Indeed, its 2.5 nm lower detection threshold has served to define the onset of new particle formation. Yet this threshold size is larger than the largest clusters analyzable by mass spectrometry.

The need to understand the transition from clusters to particle formation has motivated the development of a number of condensation particle counters with detection limits approaching 1 nm. The mixing-type, dibutylphthalate-based instruments of Gamero-Castano and

Fernandez de la Mora (2000) and of Sgro and Fernandez de la Mora (2004) have detection limits near 1.2 nm. The instrument developed by Iida et al. (2009) was the first to extend laminar-flow condensation particle counting into the sub-2 nm size range. Through systematic evaluation of the physical properties of candidate working fluids, Iida et al. introduced the use of diethylene glycol to activate condensational growth followed by a normal butanol-based “booster” CPC to enlarge the droplets to readily detectable sizes. Atmospheric measurements with this instrument operated with a mobility separator, combined with data from a cluster chemical ionization mass spectrometer, yielded the first reported continuous size distributions in the sub-2 nm size range, from molecular clusters with mass equivalent diameters in the 0.6–1 nm range, to particles at 1 nm and larger (Jiang et al. 2011a,b).

Following on the work of Iida et al. on the use of diethylene glycol, and the work of Sgro and Fernandez de la Mora on mixing designs, Vanhanen et al. (2011) introduced a mixing type CPC using diethylene glycol,

again coupled to a butanol-based booster. More recently, Kuang et al. (2012) and Kangasluoma et al. (2015), pushed the detection limits of the laminar-flow butanol-based instruments to near 1 nm through a combination of larger temperature differences and higher flow rates. These instruments take advantage of the slower rate for the formation of butanol clusters through homogeneous nucleation, as compared to the heterogeneous condensation of butanol vapor onto particles. Another approach is the adiabatic expansion used in the vSANC, which may be used with a variety of condensable working fluids, and has recently shown detection near 1 nm (Pinterich et al. 2016).

There continues to be the need for water-based, laminar-flow condensation particle counters with detection limits approaching 1 nm. Condensation with water is of interest as differences in activation by water and diethylene glycol or butanol can reveal information about particle chemistry, as shown in the CPC battery of Kumala et al. (2007) and Kangasluoma et al. (2014). Further, as pointed out by Sgro and Fernandez de la Mora (2004), by Iida et al. (2009) and by Fernandez de la Mora (2011), those condensing materials with high surface tension (such as water) can attain smaller activation size before triggering homogeneous nucleation. Laminar flow is of interest as the distribution in the peak saturation ratio along each flow trajectory is narrow, and well-defined. Also, for the same temperatures, the differential rates of thermal and mass diffusion that characterizes laminar flow systems produce higher supersaturations than perfect mixing.

Reported here is a new type of water-based, laminar flow condensation particle counter that is compact, relatively simple, and capable of particle detection near 1 nm. This new instrument employs an unsheathed, laminar-flow growth tube with three temperature regions: a cooled conditioner, a short, hot wet-walled section to initiate the condensational growth, followed immediately by a cooled section. This final cooled section reduces the temperature and water content of the exiting flow while maintaining supersaturated conditions (Hering et al. 2014). Use of a third stage effectively decouples the condensational growth process from water vapor content of the output flow, which in turn eliminates vapor condensation in the unheated transport lines, and makes feasible operation at the large temperature differences necessary to create high supersaturations. Further, it permits the optics to run at much cooler temperatures than for the commercially available 2-stage, laminar flow water condensation particle counters (Hering et al. 2005; Iida et al. 2008), and provides user flexibility in the selection of the temperature differences that control the peak supersaturation, and hence the particle size detection limits. We refer to this new instrument as a “versatile” water

condensation particle counter, or vWCPC, due to the flexibility it offers in the range of operating temperatures, and hence in the peak supersaturation achieved.

In this work we present application of this three-stage vWCPC to the detection of particles approaching 1 nm in diameter. The instrument is calibrated using mobility-selected particles with comparison to an electrometer. In addition, we evaluate the detection of ions generated when passing air through a bipolar source, and we examine the vWCPC time response. Each of these factors is important to size distribution measurements in ambient aerosols.

Instrument description

The condensational growth tube of the vWCPC consists of a single, wet-walled tube with three temperature regions. These three regions are referred to as a “conditioner,” “initiator” and “moderator.” The “conditioner” has cold walls, and serves much like those used in prior water-based condensation particle counters to bring the flow to saturation at a desired, cool temperature (Hering and Stolzenburg 2005). This is followed by a short, hot-walled “initiator,” that adds the water vapor for particle activation. The initiator is only long enough for the supersaturation to achieve its maximum centerline value, and is too short to warm the central portion by more than a fraction of the initiator-conditioner temperature difference. This is followed by longer “moderator” stage that again is cooled. The moderator lowers the temperature and water content of the output flow while maintaining the supersaturation needed for particle growth (Hering et al. 2014).

Details are shown in Figure 1. Flow enters the vWCPC inlet at ~ 2.2 L/min, from which a sample flow

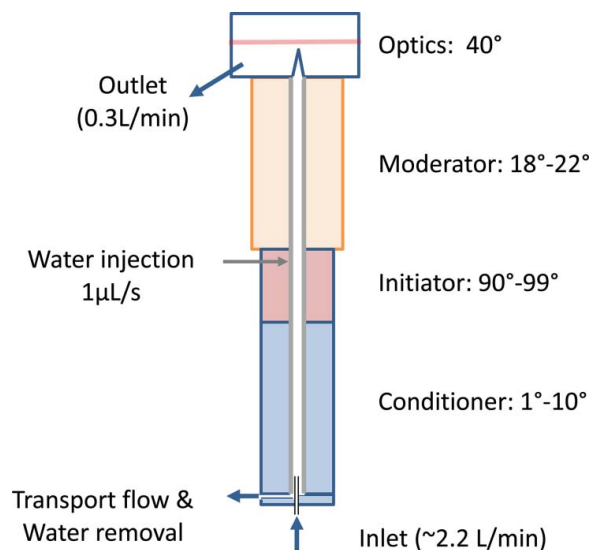


Figure 1. The versatile water condensation particle counter.

of 0.3 L/min is extracted. This sample flow is directed upward through the wet-walled growth tube which contains a single wetted wick that spans the conditioner, initiator and moderator sections. The temperature of each section is controlled independently. For tests presented here the conditioner walls are cooled to 1°–10°C, the initiator walls are heated to 90°–99°C, and the moderator walls are cooled to 18–22°C. The optics are held at 40°C. Total length is 180 mm, of which the warm initiator is 20% of the total length, and the conditioner and moderator stages are each 40%. The wick is formed by rolling an autoclavable membrane filter media (Durapore DVPP, Merk Millipore). It has an internal diameter ~ 6 mm, which is a compromise between the narrow wick needed to reduce concentration effects and the wider wick that gives longer time in the region of maximum supersaturation, as needed to induce particle activation (Lewis and Hering 2013). Liquid water is introduced into the initiator stage at a rate of 1 $\mu\text{L/s}$ using a syringe pump (Cavro, Tecan Group Ltd., Männedorf, Switzerland). Excess liquid water accumulates at the bottom of the wick (at the entrance of the conditioner) and is exhausted with the transport flow. This prototype system was implemented using the optics and motherboard from a TSI model 3783 (TSI Inc., Shoreview, MN, USA).

Experimental methods

The vWCPC was evaluated using metal oxide particles generated from resistively heating a nichrome wire in air (Kangasluoma et al. 2015), using a generator constructed by one of the authors (attoui@u-pec.fr), and subsequently size-selected using a “half mini DMA” high-resolution differential mobility analyzer (Fernandez de la Mora and Kozlowski 2013; NanoEngineering Corp., West Palm Beach, FL, USA). The half-mini DMA was operated in recirculating mode, using an Ametek blower and a HEPA cartridge filter. Particle sizing was confirmed using electrosprayed tetraheptyl ammonium bromide (THABr, monomer mobility size 1.47 nm, Ude and Fernandez de la Mora 2005). Absolute pressure immediately upstream of the vWCPC was approximately 90 kPa. The half-mini DMA was operated with the “long bullet” which provides a 20 mm longitudinal separation between aerosol inlet and outlet slits, and allows particle

size selection from 1–7 nm. The vWCPC characterization was extended to 15 nm using the TSI nano-DMA (TSI Model 3080). Concentrations of the monodispersed particles from the heated wire ranged from 10^3 to 10^4 cm^{-3} for those carrying positive charge, and from 10^2 to 10^4 cm^{-3} for those with a negative charge.

As shown in Figure 2, the monodispersed particle flow from the differential mobility analyzer was divided between the vWCPC and an electrometer built by Fachhochschule Nordwestschweiz (FHNW). The electrometer was operated at 5 L/min, which is twice the inlet flow to the vWCPC. To balance diffusional losses, the lengths of transport lines were chosen to be proportional to flow. Specifically, the distance from the flow split to the Faraday cup of the electrometer, including internal plumbing within the electrometer, was fixed at 24 cm, while that to the vWCPC was 12 cm. Both transport lines contained one 90 degree bend. Aerosol and electrometer flows were monitored with mass flow meters (TSI Inc.) and checked at room inlet pressure against a bubble flow meter (Gilibrator, Sensidyne). With these flows the electrometer signal at the lowest particle concentrations (100 cm^{-3}) was 5 times higher than the noise level. Additionally, a set of calibration checks were done using a TSI electrometer (Model 3068B) that was provided to us by TSI, and calibrated by TSI immediately prior to these experiments.

In addition to the wire-generated aerosols, tests were done with charger ions, and with ammonium sulfate, sodium chloride and sucrose containing particles. The term “charger ions” refers to the trace gases in ambient air that become charged when exposed to a bipolar ion source (Kangasluoma et al. 2013). Tests conducted here used filtered laboratory air that was passed through a soft X-ray bipolar ion source (TSI Model 3087). Zero counts and ion detection was determined through switching on and off the X-ray source. Experiments were also done with mobility selected charger ions using the DMA.

Sulfate-containing particles were generated using a 300°C tube furnace into which an airflow containing charge-neutralized atomized ammonium sulfate was introduced. A 48-month old Po source (NRD 2U500 Staticmaster) was used to introduce charge onto the particles exiting the furnace, while limiting the concentration of ions mixed

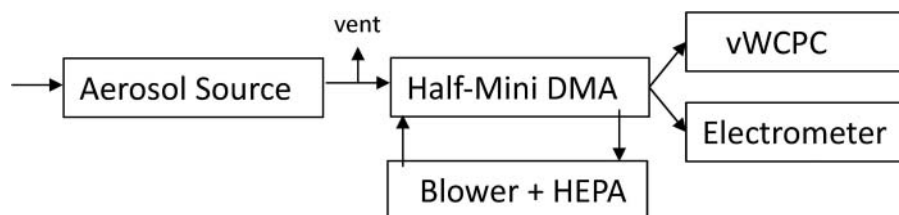


Figure 2. Experimental configuration.

in with the aerosol. A similar approach was used to generate particles containing sodium chloride, with an atomizer feeding a 650°C oven. Separate tubes were used for the sulfate and sodium chloride generation. Concentrations ranged from 10^2 cm^{-3} near 1 nm to a broad maximum of 3500–7500 at 3–4 nm. Sucrose was generated using an electrospray that incorporated a new Po source (NRDP-2042 Nuclepot). In positive mode, concentrations peaked at $2 \times 10^4 \text{ cm}^{-3}$ at 1.6 nm, and in negative mode concentrations peaked at 10^4 cm^{-3} at 1.0 nm, similar to that found for charger ions alone. Above 2 nm, concentrations varied from 200–1000 cm^{-3} .

The time response of the system was examined by counting the digital pulses from the vWCPC in 20 ms intervals. Experiments were done four ways. In the first approach (Method 1), a filter placed on the inlet was simply removed by hand as rapidly as possible, while a small fan blew air across the inlet. Method 2 used solenoid valves to switch between laboratory and filtered air streams. Method 3 used an electrospray source positioned immediately below the vWCPC inlet, with filtered air blowing across the inlet, giving near-zero counts until application of the field to start the electrospray. All three of these approaches tracked the rise from zero, or near-zero concentration to a steady plateau. The last approach, Method 4, used a spark generator from a spent household barbecue lighter. This was placed near the inlet to provide a sharp “delta function” peak in particle concentration, as described by Wang et al. (2002). In all instances the raw count data were converted to particle number concentrations by applying the particle count rate dead time correction measured separately for this vWCPC. Only data with peak concentrations below $8 \times 10^4 \text{ cm}^{-3}$ were used.

Results

Response to charger ions

Depending on the application, sensitivity of particle condensation counters to molecular ions is either helpful, or not desired. For aerosol size distributions measurements, detection of ions is problematic. The bipolar ion sources such as Po, Am or soft X-ray “neutralizers” used in conjunction with aerosol mobility measurements produce an abundance of ions with mobility values in the 1–2 nm size range. Mobility-based particle size distribution measurements in this sub-2 nm size range require that the condensation particle counter used as a detector be insensitive to these charger ions, while simultaneously detecting particles at the same mobility. On the other hand, mobility size analysis of large molecules requires sensitivity to these molecular ions.

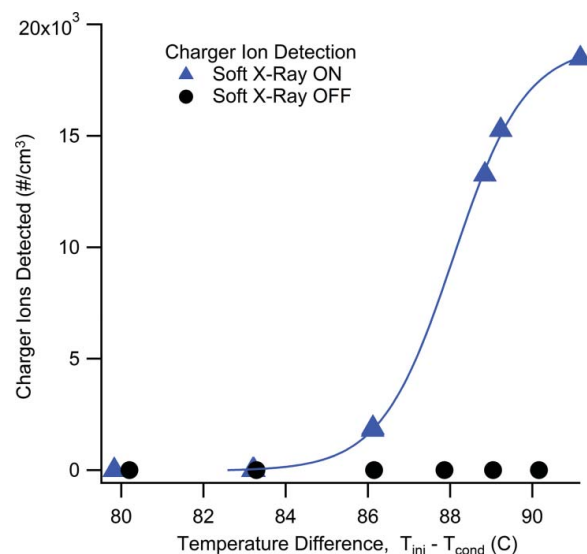


Figure 3. Response of the vWCPC to ions produced from passing filtered room air through a soft X-Ray ion source, as a function of the temperature difference between the Initiator and the Conditioner (triangles). Comparison is given to operation with the Soft X-ray in place, but turned off so as not to generate ions (circles). Tests were done with the initiator at 90–91°C.

Figure 3 shows the response of the vWCPC to ions from a soft X-ray bipolar ion source introduced into filtered laboratory air. Data are shown as function of the temperature difference between the first two stages, where the initiator temperature was held at 90°C, while the conditioner temperature was increased from 1 to 10°C (the moderator stage was $18 \pm 1^\circ\text{C}$). For operation at 10° and 90° (80°C temperature difference), the count rate by the vWCPC was the same with, or without ions, at 10^{-3} cm^{-3} . At temperature difference of 86°C, the vWCPC starts to respond to the charger ions with count rates increasing to 10^4 cm^{-3} at 90°C.

To determine the detection efficiency for charger ions, measurements were also done with mobility classified charger ions, as shown in Figure 4. When operated at the largest temperature differences, with the conditioner set to 1°C and the initiator set to 99°C, the positive ions produced by the Po source in our electrospray were detected with an efficiency of 5–10%. Detection of the negative ions ranged from 10–20%. These charger ions are dominated by small volatile organic compounds (Kangasluoma et al. 2013), which likely are not readily activated by water (Hering et al 2005).

Response to wire-generated particles

The size response of the vWCPC was examined for three sets of temperature conditions: (i) 10° and 90°C, (ii) 2° and 90°C, and (iii) 1° and 99°C for the conditioner (T_c) and initiator (T_i), respectively. The first of these settings

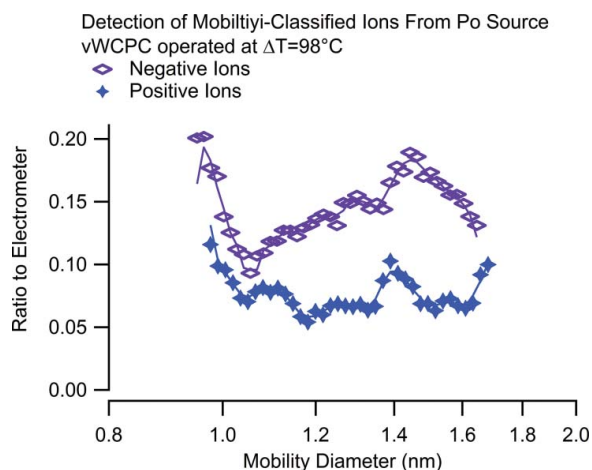


Figure 4. vWCPC detection efficiency for mobility-selected ions obtained from passing filtered laboratory air through a Po ion source. The vWCPC is operated at conditioner and initiator temperatures of 1°C and 99°C, respectively.

(10° and 90°C) is selected for evaluation because of its insensitivity to charger ions. The larger temperature differences are tested because of the potential for detection of yet smaller particle sizes.

Results are shown in Figure 5 for positively and negatively charged particles generated from the heated nichrome wire. For the 80°C temperature differential that is insensitive to charger ions ($T_c = 10^\circ\text{C}$, $T_i = 90^\circ\text{C}$), the vWCPC reaches 50% of the electrometer reading at 1.9 nm mobility diameter for both positively and negatively charged particles from the heated nichrome. The curve rises to above 90% at 4 nm. At the largest temperature differential settings tested, with $T_c = 1^\circ\text{C}$ and $T_i = 99^\circ\text{C}$, the vWCPC electrometer ratio reaches 50% at a mobility diameter of 1.6 nm. Correcting for the

gas molecular diameter (Ku and Fernandez de la Mora 2009), the physical particle diameter at this cut-point is 1.3 nm. The inlet pressure during these tests was 90 kPa, for which the boiling point of water is 95°C. Thus it is likely that the temperature of the wick at the initiator was closer to 95°C for these tests. Figure 5 also shows results for somewhat more moderate temperatures of $T_c = 2^\circ\text{C}$ and $T_i = 90^\circ\text{C}$ for which the detection efficiency curves are nearly identical to the 1° and 99°C setting.

For a subset of the tests, a TSI Model 3890B electrometer was available. Figure 5 compares the efficiency curves obtained when using this TSI electrometer in place of the FHNW electrometer that served as reference for the other measurements presented here. As shown, the data obtained with the two electrometers are quite comparable. For negatively charged particles the curves differ in the 1.9–2.4 nm range, but the particle size at 50% detection is the same. For positively charged wire-generated particles the curves are essentially identical. This comparison lends confidence to the measurements presented here.

At each of the three operating conditions, the measurements with the wire-generated particles were extended to 13 nm using the TSI nano-DMA for size selection. These data, shown in Figure 5, reveal an extension to larger particle sizes of the plateau attained near 4 nm. While the asymptotic value is reasonable, the puzzling aspect is that this plateau should be achieved at such a small particle size. One would expect diffusional losses in the conditioner would affect the efficiencies. The laminar flow relations predict 3% loss at 7 nm, and 12% loss at 4 nm. While there could be size-dependent losses in the electrometer measurement that served as reference, the good comparison with the

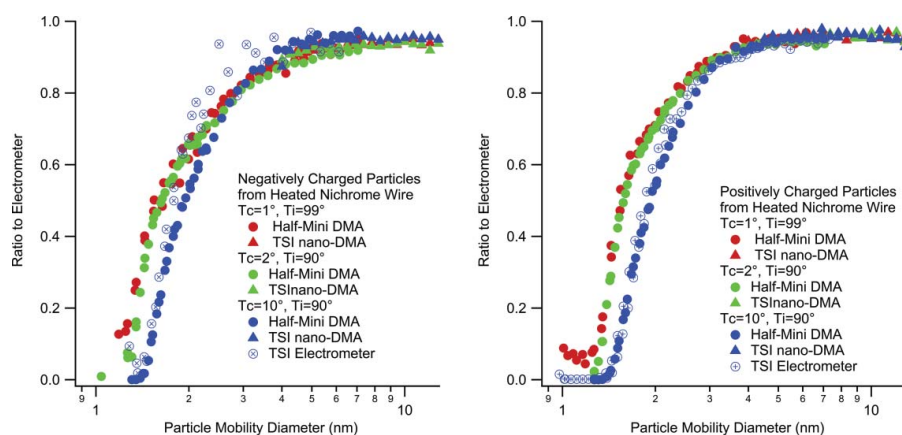


Figure 5. Response of the vWCPC to negatively and positively charged particles from a heated nichrome wire at three sets of operating temperatures for the conditioner (T_c) and initiator (T_i), as shown. Calibrations below 7 nm were obtained with the Half-mini DMA, while those from 5 to 12 nm are from the TSI nano-DMA. Open symbols indicate data obtained using the TSI electrometer as reference. All other data were obtained using the FHNS electrometer.

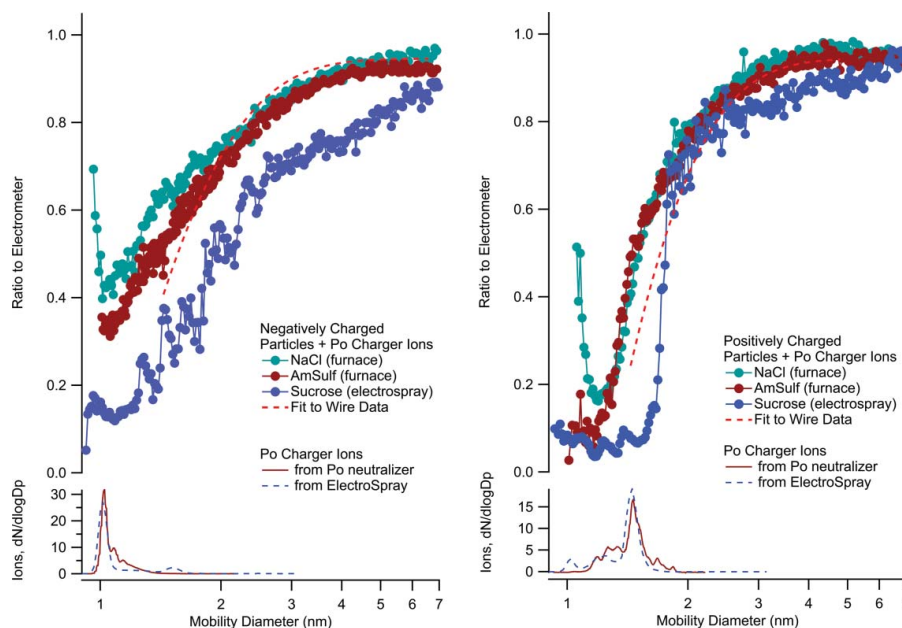


Figure 6. Response of the vWCPC to ammonium sulfate, sodium chloride, and sucrose containing particles, mixed with charger ions. Also shown is the mobility spectrum of the charger ions in the absence of particles. Operating temperatures of the vWCPC were 1° and 99°C for the conditioner and initiator, respectively.

TSI electrometer would argue otherwise. Resolution of this issue awaits further investigation.

Response to other particle types

Figure 6 presents results for three other types of particles, sulfate and sodium chloride containing particles generated using a furnace, and sucrose generated by electrospray. For reference, fits through the nichrome wire data of Figure 5 are included. These data are at the highest temperature difference tested, with conditioner and initiator set points of 2°C and 99°C. They are complicated by the presence of charger ions, which are abundant, and detected by the electrometer, but only seen at <20% efficiency by the vWCPC. The mobility distributions measured for the Po charger ions alone, in the absence of particles, is also shown. However, it is not possible to correct the data for the charger ions because their concentration in the presence of the particles is not known.

Although our test aerosols surely contained unknown contaminants, compositional differences are apparent. These differences are most readily seen in the negative mode spectrum, for which the charger ions are mostly found near 1 nm. The sodium chloride containing particles are detected more efficiently than those with sulfate, much as seen in the first water-based condensation particle counters (Hering et al. 2005). The upturn in the detection of positively charged sodium chloride near 1 nm could be due to the decrease in the charger ion concentration at sub-1 nm sizes. The detection efficiency

for the sucrose is lower than for either the sodium chloride or sulfate containing particles for particles below 7 nm. The wiggles in the sucrose detection spectrum are attributed to the presence of sucrose clusters, which are seen more readily than the charging ions (Kaufman and Dorman 2008). These wiggles are also visible in the electrometer data for the negatively charged sucrose. The positive mode data are more difficult to interpret due to the presence of the charging ions. Results are similar for sodium chloride and sulfate above 1.3 nm, while at smaller sizes the sodium chloride containing particles are more readily detected. Again, we see wiggles in the sucrose spectrum. The efficiency rises sharply once as the mobility size increases above that of the charger ions.

In all of these experiments, homogeneous nucleation of water vapor was never detected. At elevated temperatures of 1° and 99°C, the background particle count rate observed when sampling filtered air was $<0.1 \text{ cm}^{-3}$, even at reduced inlet pressures. However, at these higher temperature differences, placement of a Kr-85 source outside the instrument, but in the proximity of the initiator, produced particle counts of the order of 100 cm^{-3} , possibly as a result of gamma-ray induced ion nucleation.

Time response

Figure 7 shows results for the instrument response time derived from the rapid removal of a filter placed at the inlet (test Method 1). Data are plotted as $1-(N(t)/N_f)$, where $N(t)$ is the time-dependent number concentration,

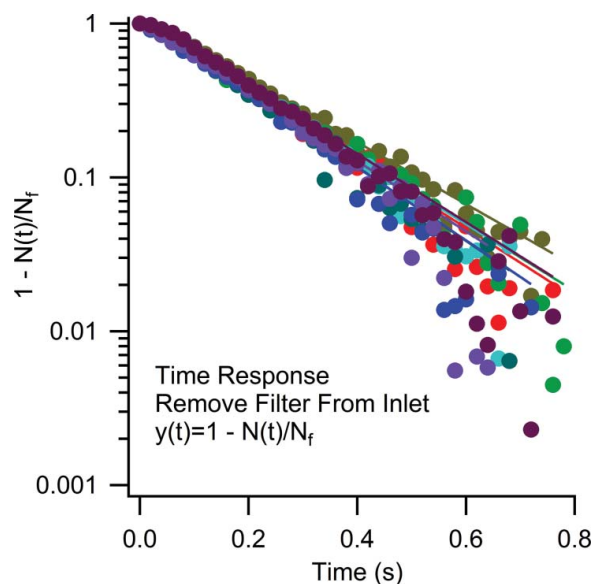


Figure 7. Time response of the vWCPC, shown as the particle concentration normalized with respect to the final concentration, when quickly removing a filter from the inlet. Shown are seven separate tests, each indicated by a different symbol.

rising from zero to a final concentration of N_f . The time constant τ was evaluated for each run assuming an exponential rise in concentration, i.e., $1 - N(t)/N_f = A_{\text{exp}}(-t/\tau)$. Even though this approach involved manual removal of the inlet filter, the results were consistent, with 19 tests yielding $\tau = 195 \pm 9$ ms. This is similar to the value of $\tau = 175$ ms measured by Wang et al. (2002) for the TSI-3025 butanol based instrument, which is a sheathed, laminar flow instrument, but is longer than the $\tau = 58$ ms they report for their fast mixing counter. The distribution of residence times for a laminar flow is not exactly exponential, and indeed a slight deviation from pure exponential behavior can be seen in Figure 7. For short times, the integral over the residence time distribution can be approximated by an exponential for a laminar flow, which resembles the step function change of our experiments. For the flow rate and tube length of our system ($5 \text{ cm}^3/\text{s}$, 18 cm), but neglecting the transport of water vapor to and from the walls, this exponential approximation to the integral over the residence time distribution gives a value of $\tau = 250$ ms.

When using a solenoid valve to switch between filtered and ambient room air lines (Method 2), the indicated value of τ was about 20% longer, presumably due to mixing in the transport lines after the solenoid valve. The electrospray tests (Method 3) yielded somewhat shorter, yet more variable results. It is possible that upon startup the particle concentration generated by the electrospray was higher than the plateau value, generating a higher driving force for the concentration rise than was captured by the data. Similarly, for the Method 4 spark tests, the

derived values of τ varied from 50 ms to 250 ms, with consistently longer values of τ found when the peak concentrations were higher. These variations point to the difficulty of making tests of response times when response times are relatively fast. Among these tests, Method 1, yielding a value of $\tau = 195$ ms, is our best estimate of the time constant that characterizes the response for the vWCPC, as it provides a consistent value over a range of concentrations. For this value of τ the corresponding rise time required to attain 95% of the final concentration, when subjected to a step function change, is 580 ms.

General observations

An interesting feature of the vWCPC is that when operated at initiator temperatures $\geq 90^\circ\text{C}$ temperatures, as done here, the pulse heights of droplets detected by the optics are very uniform. Generally, with the tightly focused beam of the TSI Model 3783 type optics used here, such uniformity is only observed in sheathed instruments, wherein the particles are confined along the centerline. The uniformity observed in the vWCPC pulse heights indicates that the droplets may be focused along the centerline, similar to a sheathed instrument, as if the addition of water vapor to the flow from the walls of the initiator directs particles towards the center of the flow prior to their activation. Such uniformity offers an intriguing potential for small particle “Kelvin” sizing based on pulse height, and indeed we do observe a gradual increase in mean pulse height with particle sizes in the size range below 2.5 nm for the wire-generated particles. However such analyses are complicated by the dependence of pulse height on particle concentration, and were not explored.

A key feature of the vWCPC is the incorporation of the third “moderator” stage that reduces both the temperature and the dew point of the output flow. One consequence of this extra stage is that the temperature differential that determines the peak supersaturation can be changed without adjusting the temperature of the optics. This is of practical importance as the alignment of the optics is temperature dependent. The original two-stage design of the original WCPC required the optics to be run at the temperature of the condensation region, and hence these instruments require realignment whenever adjusting this temperature. In contrast, the vWCPC the maximum supersaturation depends on the operating temperatures of the initiator and the conditioner, and is independent of the temperature of the moderator stage. Thus the optics can be run at a fixed temperature regardless of the choice of peak supersaturation desired, avoiding the need for realignment. Another advantage of the third stage is that the vWCPC

does not accumulate water condensate in its downstream flow lines. For all of the data presented above, the optics of the system were operated at a 40°C which is 20° lower than the temperature of the current general purpose, and 35° lower than the current ultrafine water-based condensation particle counters. Moreover, there is no need for an additional water separator to remove water vapor from the exit flow.

A further advance in the vWCPC design is in the water handling. A key feature that increases instrument reliability is the elimination of all internal liquid reservoirs and vent lines. In place of the gravity-feed of an internal water reservoir, water injection is handled by a pump that completely isolates the external water reservoir from the system operating pressure at all times. As a result of this design change, the system is very tolerant of pressure fluctuations at the inlet. As stated above, the calibrations were done at slightly below atmospheric pressure, at an inlet pressure of 90 kPa, as this was necessitated by our specific experimental setup. We found that no precautions were needed when quickly connecting to, or from this reduced pressure system. The instrument never flooded, even when temporarily blocking the inlet completely. This tolerance is attributed directly to use of a direct injection water feed that does not need venting lines as with internal water reservoirs. Any excess water accumulating on the surface of the wick is removed at the bottom by the 2.2 L/min transport flow, which is sufficient even at reduced pressure. Second, the continuous injection and removal of water has the effect of continually washing the wick, such that it does not accumulate salts which can degrade performance over time. These two features, developed over a decade of experience with water condensation instruments, appear to have eliminated problems of wick degradation and flooding.

Each of these features—the reduction of the optics head temperature, the minimization of the condensate in the output flow, and the elimination of vented reservoirs—contribute to a more robust instrument. The reduction in optics temperature and minimization of condensate are a direct result of the three stage “moderated” approach for laminar flow condensational growth. Further, it allows growth tube operating temperatures to be adjusted without changing the temperature, and hence alignment, of the optics. The elimination of the vented internal reservoirs further contributes to the instrument reliability and provides flexibility in operating conditions.

Conclusions

A versatile water-based condensation particle counter has been developed for which operating conditions can

be selected to either exclude the detection of ions from a bipolar charger, or to allow detection of these molecular ions. Evaluation with aerosols generated from a heated nichrome wire indicates 50% detection at 1.9 nm mobility diameter when operating to avoid detection of charger ions, and 1.6 nm mobility diameter when temperatures are boosted. Soluble inorganic ionic compounds such as ammonium sulfate and sodium chloride are detected at yet smaller particle sizes. The time response, of the order of 195 ms, is comparable to that of the sheathed laminar flow instruments such as the TSI-3025. Importantly, the vWCPC is basically a simple instrument, with no sheath flow, no internal water reservoirs and no vents required for pressure balancing. Through the three-stage approach, the temperature and water content of the exiting flow are moderated, enabling the optics to be operated at 40°C, and eliminating condensate in the exiting flow. In addition to providing sub-2 nm particle detection, the vWCPC has shown itself to be exceptionally reliable.

Acknowledgments

The authors thank TSI Inc. for providing the electrometer, optics and electronics, and we thank Brookhaven National Laboratory for supporting CK's time while working in our laboratory.

References

- Fernández de la Mora, J. F. (2011). Heterogeneous Nucleation with Finite Activation Energy and Perfect Wetting: Capillary Theory versus Experiments with Nanometer Particles, and Extrapolations on the Smallest Detectable Nucleus. *Aero. Sci. Technol.*, 45(4):543–554.
- Fernández de la Mora, J. F., and Kozlowski, J. (2013). Hand-Held Differential Mobility Analyzers of High Resolution for 1–30 nm Particles: Design and Fabrication Considerations. *J. Aero. Sci.*, 57:45–53.
- Gamero-Castano, M., and Fernández de la Mora, J. (2000). A Condensation Nucleus Counter (CNC) Sensitive to Singly Charged Sub-Nanometer Particles. *J. Aero. Sci.*, 31(7): 757–772.
- Hering, S. V., Stolzenburg, M. R., Quant, F. R., Oberreit, D. R., and Keady, P. B. (2005). A Laminar-Flow, Water-Based Condensation Particle Counter (WCPC). *Aero. Sci. Technol.*, 39(7):659–672.
- Hering, S. V., and Stolzenburg, M. R. (2005). A Method for Particle Size Amplification by Water Condensation in a Laminar, Thermally Diffusive Flow. *Aero. Sci. Technol.*, 39 (5):428–436.
- Hering, S. V., Spielman, S. R., and Lewis, G. S. (2014). Moderated, Water-Based, Condensational Particle Growth in a Laminar Flow. *Aero. Sci. Technol.*, 48(4):401–408.
- Iida, K., Stolzenburg, M. R., and McMurry, P. H. (2009). Effect of Working Fluid on Sub-2 nm Particle Detection with a

- Laminar Flow Ultrafine Condensation Particle Counter. *Aero. Sci. Technol.*, 43(1):81–96.
- Iida, K., Stolzenburg, M. R., McMurry, P. H., Smith, J. N., Quant, F. R., Oberreit, D. R., Keady, P. B., and Hering, S. V. (2008). An Ultrafine, Water-Based Condensation Particle Counter and its Evaluation Under Field Conditions. *Aero. Sci. Technol.*, 42(10):862–871.
- Jiang, J., Chen, M., Kuang, C., Attoui, M., and McMurry, P. H. (2011a). Electrical Mobility Spectrometer using a Diethylene Glycol Condensation Particle Counter for Measurement of Aerosol Size Distributions Down to 1 nm. *Aero. Sci. Technol.*, 45(4):510–521.
- Jiang, J., Zhao, J., Chen, M., Eisele, F. L., Scheckman, J., Williams, B. J., Kuang, C. and McMurry, P. H. (2011b). First Measurements of Neutral Atmospheric Cluster and 1–2 nm Particle Number Size Distributions During Nucleation Events. *Aero. Sci. Technol.*, 45(4):ii–v.
- Kangasluoma, J., Ahonen, L., Attoui, M., Vuollekoski, H., Kulmala, M., and Petäjä, T. (2015). Sub-3 nm Particle Detection with Commercial TSI 3772 and Airmodus A20 Fine Condensation Particle Counters. *Aero. Sci. Technol.*, 49(8):674–681.
- Kangasluoma, J., Kuang, C., Wimmer, D., Rissanen, M. P., Lehtipalo, K., Ehn, M., Worsnop, D., Wang, J., Kumala, M. and Petäjä, T. (2014). Sub-3 nm Particle Size and Composition Dependent Response of a Nano-CPC Battery. *Atmos. Meas. Tech.*, 7(3):689–700.
- Kangasluoma, J., Junninen, H., Lehtipalo, K., Mikkilä, J., Vanhanen, J., Attoui, M., Sipilä, D., Worsnop, Kulmala, M. and Petäjä, T. (2013). Remarks on Ion Generation for CPC Detection Efficiency Studies in Sub-3-nm Size Range. *Aero. Sci. Technol.*, 47(5):556–563.
- Kaufman, S. L., and Dorman, F. D. (2008). Sucrose Clusters Exhibiting a Magic Number in Dilute Aqueous Solutions. *Langmuir*, 24(18):9979–9982.
- Ku, B. K., and Fernández de la Mora, J. F. (2009). Relation between Electrical Mobility, Mass, and Size for Nanodrops 1–6.5 nm in Diameter in air. *Aero. Sci. Technol.*, 43(3):241–249.
- Kuang, C., Chen, M., McMurry, P. H., and Wang, J. (2012). Modification of Laminar Flow Ultrafine Condensation Particle Counters for the Enhanced Detection of 1 nm Condensation Nuclei. *Aero. Sci. Technol.*, 46(3):309–315.
- Kulmala, M., Mordas, G., Petäjä, T., Grönholm, T., Aalto, P. P., and Vehkamäki, H. (2007). The Condensation Particle Counter Battery (CPCB): A New Tool to Investigate the Activation Properties of Nanoparticles. *J. Aero. Sci.*, 38(3):289–304.
- Lewis, G. S., and Hering, S. V. (2013). Minimizing Concentration Effects in Water-Based, Laminar-Flow Condensation Particle Counters. *Aero. Sci. Technol.*, 47(6):645–654.
- Pinterich, T., Vrtala, A., Kaltak, M., Kangasluoma, J., Lehtipalo, K., Petäjä, T., Winkler, P. M., Kulmala, M., and Wagner, P. E. (2016). The Versatile Size Analyzing Nuclei Counter-vSANC. *Aero. Sci. Technol.* 50:947–958. Available at <http://dx.doi.org/10.1080/02786826.2016.1210783>
- Sgro, L. A., and Fernández de la Mora, J. F. (2004). A Simple Turbulent Mixing CNC for Charged Particle Detection Down to 1.2 nm. *Aero. Sci. Technol.*, 38(1):1–11.
- Stolzenburg, M. R., and McMurry, P. H. (1991). An Ultrafine Aerosol Condensation Nucleus Counter. *Aero. Sci. Technol.*, 14(1):48–65.
- Ude, S., and Fernández de la Mora, J. F. (2005). Molecular Monodisperse Mobility and Mass Standards from Electrosprays of Tetra-Alkyl Ammonium Halides. *J. Aero. Sci.*, 36(10):1224–1237.
- Vanhanen, J., Mikkilä, J., Lehtipalo, K., Sipilä, M., Manninen, H. E., Siivola, E., Petaja, T and Kulmala, M. (2011). Particle Size Magnifier for Nano-CN Detection. *Aero. Sci. Technol.*, 45(4):533–542.
- Wang, J., McNeill, V. F., Collins, D. R., and Flagan, R. C. (2002). Fast Mixing Condensation Nucleus Counter: Application to Rapid Scanning Differential Mobility Analyzer Measurements. *Aero. Sci. Technol.* 36(6):678–689.